
TECHNICAL REPORT

Improvement of Critical Heat Flux Correlation for Research Reactors using Plate-Type Fuel

Masanori KAMINAGA[†], Kazuyoshi YAMAMOTO and Yukio SUDO

*Japan Atomic Energy Research Institute**

(Received January 22, 1998)

In research reactors, plate-type fuel elements are generally adopted so as to produce high power densities and are cooled by a downward flow. A core flow reversal from a steady-state forced downward flow to an upward flow due to natural convection should occur during operational transients such as "Loss of the primary coolant flow". Therefore, in the thermal hydraulic design of research reactors, critical heat flux (CHF) under a counter-current flow limitation (CCFL) or a flooding condition are important to determine safety margins of fuel against CHF during a core flow reversal.

The authors have proposed a CHF correlation scheme for the thermal hydraulic design of research reactors, based on CHF experiments for both upward and downward flows including CCFL condition. When the CHF correlation scheme was proposed, a subcooling effect for CHF correlation under CCFL condition had not been considered because of a conservative evaluation and a lack of enough CHF data to determine the subcooling effect on CHF.

A too conservative evaluation is not appropriate for the design of research reactors because of construction costs *etc.* Also, conservativeness of the design must be determined precisely. In this study, therefore, the subcooling effect on CHF under the CCFL conditions in vertical rectangular channels heated from both sides were investigated quantitatively based on CHF experimental results obtained under uniform and non-uniform heat flux conditions. As a result, it was made clear that CHF in this region increase linearly with an increase of the channel inlet subcooling and a new CHF correlation including the effect of channel inlet subcooling was proposed. The new correlation could be adopted under the conditions of the atmospheric pressure, the inlet subcooling less than 78 K, the channel gap size between 2.25 to 5.0 mm, the axial peaking factor between 1.0 to 1.6 and L/De between 71 to 174 which were the ranges investigated in this study.

KEYWORDS: *critical heat flux, counter-current flow limitation, vertical rectangular channels, inlet subcooling, plate-type fuel elements, research reactors, core flow reversal, natural convection, flooding condition*

I. Introduction

For research or test reactors, plate-type fuel elements are generally adopted so as to produce high power densities in their core and are cooled down by a downward core flow. A core flow reversal from a steady-state forced downward flow to an upward flow due to natural convection should occur during operational transients such as "Loss of the primary coolant flow"⁽¹⁾. For research reactors having comparatively small thermal power, it is not necessary to credit auxiliary or emergency pumps for decay heat removal after coast-down of the main pumps in case of an emergency. Since the decay heat during a core flow reversal is low enough, there is no possibility of having a critical heat flux (CHF) condition. However, for high power research reactors have auxiliary or emergency pumps needing decay heat removal after coast-down of

the main pumps, a core flow reversal could occur under a low decay heat level with the safety margin against CHF being large enough. Therefore, in the thermal hydraulic design of research reactors, CHF under a counter-current flow limitation (CCFL) or a flooding condition including a zero flow condition is important to determine the necessity of auxiliary or emergency pumps for the decay heat removal after a reactor shut-down and to evaluate the safety margins of fuel against CHF during the core flow reversal.

The present authors have been proposed a CHF correlation scheme for the thermal hydraulic design and safety analysis of research reactors such as JRR-3 (Japan Research Reactor No. 3), based on CHF experiments for both upward and downward flows under CCFL or the flooding condition including the zero flow condition using vertical rectangular channels heated from both sides which simulate flow channels of research reactor's fuel⁽²⁾⁽³⁾. Critical heat flux correlation errors have also been made clear against the experimental data⁽²⁾⁽³⁾. When the CHF correlation scheme was proposed, a sub-

*Tokai-mura, Naka-gun, Ibaraki-ken 319-1195.

[†] Corresponding author, Tel. +81-29-282-6424,
Fax. +81-29-282-6496,
E-mail: kaminaga@jrr3fep2.tokai.jaeri.go.jp

cooling effect for a CHF correlation under a CCFL condition had not been considered because of a conservative evaluation and a lack of enough CHF data to determine the subcooling effect on CHF.

A core conversion program from high enriched uranium (HEU) fuel to low enriched uranium (LEU) fuel is currently conducted at JRR-4 (Japan Research Reactor No. 4). In the safety analysis of JRR-4, a thermal hydraulic behavior during the core flow reversal at “Loss of commercial electric power supply” was analyzed. An analytical result regarding CHF showed that the safety margin against CHF satisfied with a criterion of “the minimum DNB (departure from nucleate boiling) ratio (DNBR: maximum heat flux/DNB heat flux) should be greater than 1.5”, but the analytical result of DNBR was very close to the safety limit of 1.5. Therefore, it was required to clarify the conservativeness of the analytical result during the safety examination by the government. A too conservative evaluation is also not appropriate for the design of research reactors such as high performance new research reactors, because of construction costs *etc.* Conservativeness of the design must also be determined precisely.

In this study, therefore, the subcooling effect on CHF under the CCFL conditions in vertical rectangular channels heated from both sides were investigated quantitatively based on CHF experimental results obtained under uniform and non-uniform heat flux conditions.

II. Previous CHF Correlations

Figure 1 shows the previous CHF correlation scheme for vertical rectangular channels proposed by Sudo and Kaminaga⁽³⁾ which have been used for the thermal hydraulic design and safety analysis of research reactors using plate-type fuel such as JRR-2, JRR-3⁽⁴⁾, JRR-4⁽⁵⁾ and JMTR⁽⁶⁾ which are all operated and managed by Japan Atomic Energy Research Institute (JAERI). This CHF correlation scheme can be applicable within pressure ranges of 0.1 to 4 MPa, mass flux of -25,800 to

+6,250 kg/m²·s including stagnant flow conditions, inlet subcooling of 1 to 213 K, outlet condition extending from subcooling of 0 to 74 K to quality of 0 to 1.0 and a ratio of heated length to equivalent hydraulic diameter L/De of 8 to 240⁽³⁾.

Critical heat flux correlations included in the CHF correlation scheme are shown as follows. Equation (1) was proposed by Sudo and Kaminaga⁽³⁾⁽⁹⁾ and Eqs. (2) and (3) are originally proposed by Mishima⁽⁷⁾:

$$q_{CHF,1}^* = 0.005|G^*|^{0.611} \left(1 + \frac{5,000}{|G^*|} \Delta T_{SUB,o}^* \right) \quad (1)$$

$$q_{CHF,2}^* = \frac{A}{A_H} \Delta T_{SUB,in}^* |G^*| \quad (2)$$

$$q_{CHF,3}^* = 0.7 \frac{A}{A_H} \cdot \frac{\sqrt{W/\lambda}}{\{1 + (\rho_g/\rho_l)^{1/4}\}^2} \quad (3)$$

As shown in Fig. 1, Sudo and Kaminaga categorized CHF characteristics for rectangular channels into three regions according to the mass flux of water. In the first region, CHF is determined by a flooding condition for both upward and downward flows. In this region, the mass flux of water is comparatively low including the zero mass flux in which CHF is closely related to CCFL. This region is defined as Region I and CHF is predicted by Eq. (3). Equation (3) is a common correlation for predicting the minimum CHF for both upward and downward flows.

When the dimensionless mass flux of G^* is greater than that in the Region I, CHF for a downward flow becomes smaller than that of an upward flow. This region for upward flow is defined as Region II and CHF is predicted by Eq. (1) with $\Delta T_{SUB,o}^* = 0$. On the other hand, this region for downward flow is defined as Region II' and CHF is predicted by Eq. (2). In region II' for downward flow, CHF increases with increase of $\Delta T_{SUB,in}^*$ at same G^* as shown in Fig. 1.

When the dimensionless mass flux of G^* is greater than that in Region II, there is no difference in CHF between upward and downward flows. Critical heat flux in this region is dominated by a channel outlet subcooling. This region is defined as Region III and CHF is predicted by Eq. (1). It should be mentioned here that Eq. (2) gives the upper limits for Eq. (1) in Region III of $G^* > G_1^*$ as shown in Fig. 1 because Eq. (2) gives the condition of $\Delta T_{SUB,o}^* = 0$, and CHF in this region increases with increase of $\Delta T_{SUB,o}^*$ at same G^* as shown in Fig. 1.

G_1^* , G_2^* and G_3^* shown in Fig. 1 are region boundaries. A boundary between Region III and Region II or II' is calculated and identified as follows by using Eq. (1) with $\Delta T_{SUB,o}^* = 0$ and Eq. (2):

$$G_1^* = \left(\frac{0.005}{\frac{A}{A_H} \Delta T_{SUB,in}^*} \right)^{\frac{1}{0.389}} \quad (4)$$

A boundary between Region II and Region I is calculated and identified as follows by using Eq. (1) with

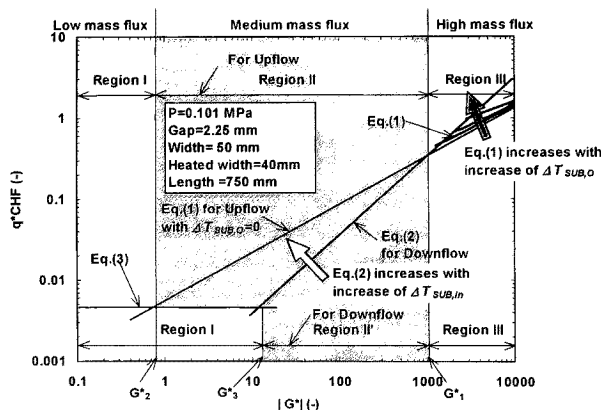


Fig. 1 Illustration of previous CHF correlation schemes for upward and downward flows in vertical rectangular channels⁽³⁾

$\Delta T_{SUB,o}^* = 0$ and Eq. (3):

$$G_2^* = \left[140 \frac{A}{A_H} \cdot \frac{\sqrt{W/\lambda}}{\{1 + (\rho_g/\rho_l)^{1/4}\}^2} \right]^{0.611} \quad (5)$$

A boundary between Region II' and Region I is calculated and identified as follows by using Eqs. (2) and (3):

$$G_3^* = 0.7 \frac{\sqrt{W/\lambda}}{\{1 + (\rho_g/\rho_l)^{1/4}\}^2 \Delta T_{SUB,in}^*} \quad (6)$$

The correlation errors of the CHF correlation scheme were estimated within -33% compared with the experimental results⁽²⁾⁽³⁾. Therefore, it was proposed that when this CHF correlation scheme was applied, the minimum DNBR should be larger than 1.5, which is equivalent to the correlation error of -33%, in the core thermal hydraulic design and safety analysis.

In the following chapter, the effect of channel inlet subcooling on CHF was investigated experimentally and Eq. (3) was selected as the base correlation to evaluate the effect of $\Delta T_{SUB,in}^*$. Because Eq. (3) was introduced based on the flooding phenomena with saturated water⁽⁷⁾ and was used as the design correlation of research reactors⁽⁴⁾⁻⁽⁶⁾ so far.

III. New CHF Correlation

Major experimental conditions of existing CHF tests⁽²⁾⁽⁸⁾ investigated in this study are listed in Table 1. All of the tests listed in Table 1 were carried out under the atmospheric pressure conditions at the channel out-

Table 1 Experimental conditions of existing CHF tests⁽²⁾⁽⁸⁾

Coolant	Water
Mass flux	0 to -73 kg/m ² (Downward) (0: stagnant flow condition)
Inlet subcooling	0 to 78 K
Channel gap size	2.25 to 5.0 mm
De	4.3 to 9.1 mm
L/De	71 to 174
Axial heat flux distribution	Non-uniform and uniform
Axial peaking factor	1.0, 1.42, 1.43, 1.6
Total number of data	69

let. Detailed information of test sections used in previous studies are shown in Table 2. A schematic of the CHF test rig and a cross-section of the test sections used in these experiments are shown in Figs. 2 and 3, respectively. It should be mentioned here that there are plena at the top and bottom of the test section as shown in Fig. 2. Because the flow channels are generally submerged in a water pool in research reactors. Axial heat flux distributions investigated in this study are shown in Fig. 4. As shown in Fig. 3, the test section simulates one sub-channel of a plate-type fuel element. Case 1 shown

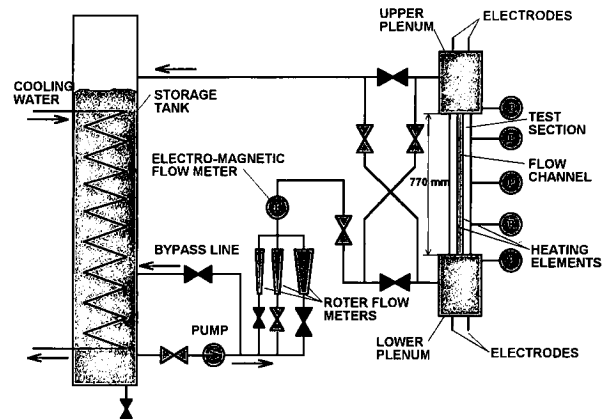


Fig. 2 Schematic of CHF test rig⁽²⁾⁽⁸⁾

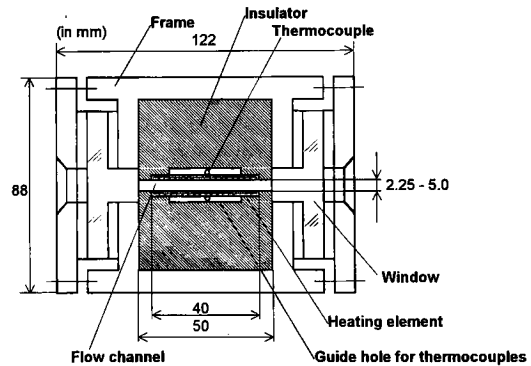


Fig. 3 Detailed cross-sectional view of test section⁽²⁾⁽⁸⁾

Table 2 Detailed information for test sections of existing CHF tests⁽²⁾⁽⁸⁾

Type	Dimension of channel (mm) width (heater width) × gap × length	Axial peaking factor	Number of CHF data	Axial heat flux distribution (see Fig. 4)
Rectangular channel	50(40) × 2.25 × 750	1.43	12	Case 1
	50(40) × 2.25 × 750	1.42	10	Case 2
	50(40) × 2.25 × 750	1.60	14	Case 3
	50(40) × 2.25 × 750	1.00	4	Uniform
	50(40) × 5.0 × 750	1.00	23	Uniform
	50(40) × 2.8 × 375	1.00	6	Uniform

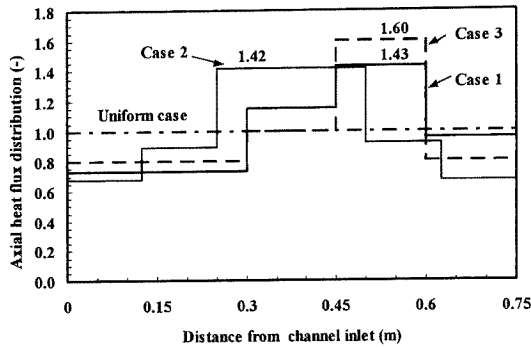


Fig. 4 Axial heat flux distributions of test sections

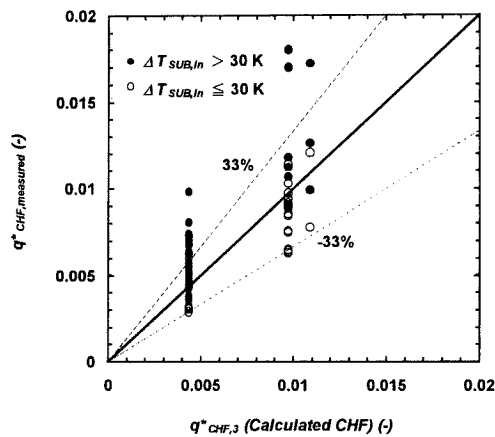


Fig. 5 Comparison with CHF experimental data for $\Delta T_{SUB,in} \leq 30\text{ K}$, $\Delta T_{SUB,in} > 30\text{ K}$ and CHF predicted by Eq. (3)

in Fig. 4 simulates a typical axial heat flux distribution of the JRR-3 core, Case 2 corresponds to a cosine curve and Case 3 is a typical axial heat flux distribution of the JRR-4 core.

Figure 5 shows comparisons between CHF predicted by Eq. (3) and all of the CHF data listed in Table 1 (69 points of data). Experimental data are classified as two groups of $\Delta T_{SUB,in} > 30\text{ K}$ and $\Delta T_{SUB,in} \leq 30\text{ K}$, to show the differences in CHF regarding the channel inlet subcooling. For non-uniform heat flux cases, the maximum heat flux was used as CHF. Because almost all of the CHF conditions occurred in the maximum heat flux region along the channel. As shown in Fig. 5, almost all the experimental data are greater than CHF predicted by Eq. (3) when the channel inlet subcoolings of $\Delta T_{SUB,in}$ are greater than 30 K. Critical heat flux predicted by Eq. (3) seems to be conservative for the CHF data which have the channel inlet subcooling of more than 30 K. The -33% line shown in the figure is the correlation error of Eq. (3) which has been evaluated in the previous study⁽²⁾. The $+33\%$ line is shown as a reference. The value of -33% was defined so that no data was less than the value predicted by Eq. (3) with

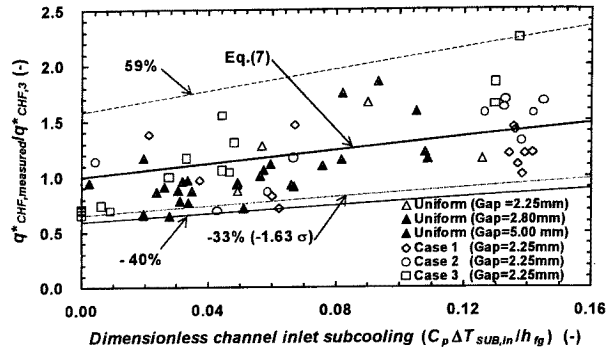


Fig. 6 Effect of channel inlet subcooling on CHF

considering the error of -33% .

Figure 6 shows all of the CHF data to make clear an effect of channel inlet subcooling on CHF in the low mass flux region where dimensionless mass flux of G^* less than G_3^* which is calculated by Eq. (6), taking $q_{CHF,measured}/q_{CHF}$ predicted by Eq. (3) as the ordinate and dimensionless inlet subcooling of $\Delta T_{SUB,in}^* [=Cp\Delta T_{SUB,in}/h_{fg}]$ as the abscissa. For the non-uniform heat flux cases, the maximum heat flux was used as CHF.

As shown in Fig. 6, CHF increased with increasing $\Delta T_{SUB,in}^*$ for both uniform and non-uniform heat flux cases although the experimental data scattered widely. A straight bold line shown in the figure was obtained based on the method of least squares under following assumptions and was expressed in the form of Eq. (7).

- (a) CHF increases linearly with an increase of $\Delta T_{SUB,in}^*$.
- (b) When $\Delta T_{SUB,in}^*$ is equal to zero under the condition of $G^* < G_3^*$, q_{CHF}^* is expressed by Eq. (3):

$$\frac{q_{CHF}^*}{q_{CHF,3}^*} = 1 + C \cdot \Delta T_{SUB,in}^* \quad (7)$$

where $C=3.0$.

Constant C in Eq. (7) was obtained by using all of CHF data shown in Fig. 6, so that Eq. (7) could predict CHF best to all of CHF data. Allowing the errors of 59% to the upper limit and 40% to the lower limit of the CHF data, Eq. (7) gives a good prediction.

In the thermal hydraulic design of research reactors, a criterion of “the minimum DNBR should be greater than 1.5” is currently adopted for both normal operation conditions and anticipated operational transients to ensure the safety of fuel against CHF. A value of 1.5 corresponds to the correlation error of -33% which have been evaluated for Eqs. (1)–(3)⁽²⁾⁽³⁾. For adopting the same criterion regarding CHF to the thermal hydraulic design of research reactors in case of Eq. (7) is selected, the confidence level of Eq. (7) to the CHF data with a deviation of -33% was investigated by the statistics analysis under an assumption that a distribution of the CHF data was the normal distribution. As a result, the deviation of -33% from Eq. (7) was evaluated to be -1.63 times of the standard deviation (-1.63σ) of the CHF data against

Eq. (7). The confidence level of the mean was estimated to be about 90% from the result of -1.63σ . This result means that there is a 10% of possibility to occur the CHF condition even when the minimum DNBR is equal to 1.5.

Equation (7) can be rewritten as follows by using Eq. (3):

$$q_{\text{CHF},3\text{NEW}}^* = 0.7 \frac{A}{A_H} \cdot \frac{\sqrt{W/\lambda}}{\{1 + (\rho_g/\rho_l)^{1/4}\}^2} \cdot \{1 + C \cdot \Delta T_{\text{SUB},in}^*\}, \quad (8)$$

where $C=3.0$.

In this study, a new CHF correlation of Eq. (8) was thus proposed. An upper limit of mass flux of Eq. (8) for the upward flow *i.e.*, a boundary between Region II and Region I, is calculated and identified as follows by using Eq. (1) with $\Delta T_{\text{SUB},o}^* = 0$ and Eq. (8):

$$G_{2,\text{NEW}}^* = \left[140 \frac{A}{A_H} \cdot \frac{\sqrt{W/\lambda}}{\{1 + (\rho_g/\rho_l)^{1/4}\}^2} \cdot (1 + 3 \cdot \Delta T_{\text{SUB},in}^*) \right]^{0.611}, \quad (9)$$

An upper limit of mass flux of Eq. (8) for the downward flow *i.e.*, a boundary between Region II' and Region I is calculated and identified as follows by using Eqs. (2) and (8):

$$G_{3,\text{NEW}}^* = 0.7 \frac{\sqrt{W/\lambda}}{\{1 + (\rho_g/\rho_l)^{1/4}\}^2} \cdot \frac{1 + 3 \cdot \Delta T_{\text{SUB},in}^*}{\Delta T_{\text{SUB},in}^*}. \quad (10)$$

Figure 7 shows comparisons between CHF predicted by Eq. (8) and all of the CHF data investigated in this study. For the non-uniform heat flux cases, the maximum heat flux was used as CHF in the same way as previous figures. The +59% and -40% lines shown in the figure are the upper and lower limits of the CHF data against Eq. (8). The -33% line shown in the figure corresponds to -1.63 times of the standard deviation (-1.63σ) of the CHF data against Eq. (8). In Fig. 7, the CHF data are also shown as two groups of $\Delta T_{\text{SUB},in} > 30$ K and $\Delta T_{\text{SUB},in} \leq 30$ K as same as those shown in Fig. 5 to clarify the differences between Eqs. (3) and (8). The channel inlet subcooling of 30 K corresponds to the dimensionless channel inlet subcooling of about 0.056 under the atmospheric pressure condition. In the case of $\Delta T_{\text{SUB},in} \leq 30$ K, differences in predicted CHF between Eqs. (3) and (8) are not so significant because of less subcooling. The differences in predicted CHF between Eqs. (3) and (8) increase with an increase of the channel inlet subcooling. As shown in Fig. 7, Eq. (8) gives much better prediction than that predicted by Eq. (3).

Figure 8 shows the CHF data obtained under uniform and non-uniform heat flux conditions with channels which have a same gap size of 2.25 mm to make

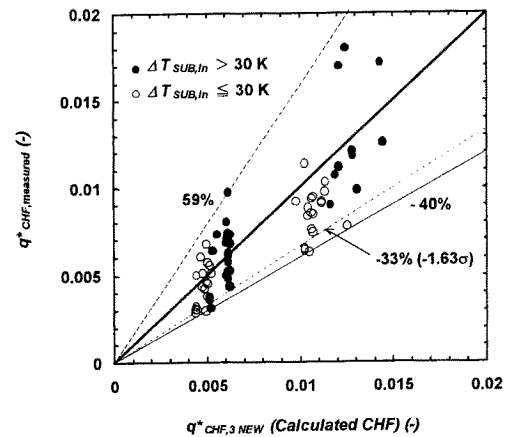


Fig. 7 Comparison between all the experimental results and CHF predicted by the new CHF correlation of Eq. (8)

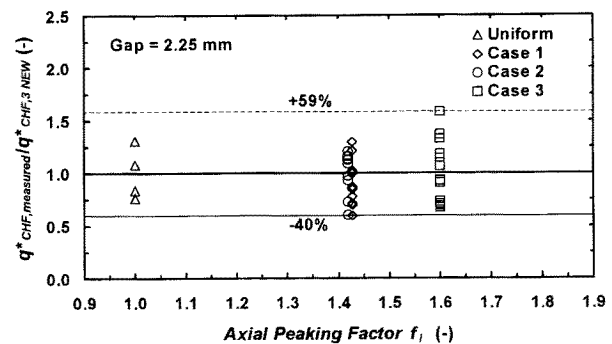


Fig. 8 Effects of axial heat flux distribution and peaking factor for CHF

clear the effects of axial heat flux distribution and peaking factor (=maximum heat flux/average heat flux) on CHF, taking an axial peaking factor as the abscissa and $q_{\text{CHF},\text{measured}}/q_{\text{CHF}}^*$ predicted by Eq. (8) as the ordinate. The +59% and -40% lines shown in the figure are the upper and lower limits of the CHF data against Eq. (8). For the non-uniform heat flux cases, the maximum heat flux was used as CHF. As already described above, almost all of the CHF conditions occurred in the maximum heat flux region along the channel. But the CHF conditions also occurred below the maximum heat flux region for some cases. In Case 1, the CHF conditions occurred in the region where the ratio of the heat flux to the average heat flux of 1.15 for two data points. In Case 2, the CHF condition occurred in the region where the ratio of the heat flux to the average heat flux of 0.90 for one data point. In Case 3, the CHF conditions occurred in the region where the ratio of the heat flux to the average heat flux of 1.00 for five data points. For these data points, use of the maximum heat flux as CHF result in over estimation of CHF compared with use of the actual heat flux in the region where the CHF occurred. Critical heat flux for these data points were overestimated 1.23 times for Case 1, 1.57 times for Case 2 and 1.60 times for

Case 3. Therefore, the CHF data for non-uniform heat flux cases shown in the figure scattered widely compared with those for uniform heat flux case. From the facts described above, it could be concluded that there were no effects of axial heat flux distribution and peaking factor regarding CHF within the ranges investigated in this study.

IV. Application to Safety Analysis of Research Reactors

In the design of research reactors, safety criteria to show whether the postulated anticipated operational transients will terminate safely or not, are defined as follows, taking into account the criteria of LWR and the characteristics of the research reactors.

- (a) The minimum DNBR shall be greater than 1.5.
- (b) The maximum fuel temperature shall not be over the blistering temperature (673 K).
- (c) Fuel plates shall not be deformed significantly by thermal stress.
- (d) The pressure in the primary cooling system shall not be over 1.1 times the design pressure.

Anticipated operational transient must be terminated before the reactor core is damaged in order to continue a normal operation condition after the anticipated operational transient. Criterion (a) is defined to prevent any burnout of fuel by a power-cooling mismatch. The minimum DNBR 1.5 is defined by considering the correlation's error against experimental data as described in Chap. II. Criterion (b) limits the fuel temperature increase in case of a big reactivity insertion, where criterion (a) is satisfied in some cases. The temperature limit of 673 K is defined as the non-blistering temperature of

uranium-aluminum (UAl_x -Al) dispersion type fuel (aluminaide fuel) and uranium-silicon-aluminum (U_3Si_2 -Al) dispersion type fuel (silicide fuel). Criterion (c) prevents a fuel rupture or decrease in coolability due to a deformation in the fuel plates due to thermal stress, *etc.* It is defined that the deformation would take place when the stress in fuel plate overcome the yield strength. Criterion (d) prevents a pressure increase in the primary cooling system which leads to component damage.

In the safety analysis of JAERI's research reactors, DNB heat flux is defined as a heat flux calculated by CHF correlations of Eqs. (1), (2) and (3), even though the CHF condition is not caused by DNB. **Table 3** shows analytical results of the anticipated operational transients for the JRR-4 silicide fueled core. As shown in Table 3, the most severe case is "Loss of commercial electric power supply" from the viewpoint of DNBR and only in this case, Eq. (3) was used to predict CHF during core flow reversal. As for JRR-3, a core flow reversal is also expected at "Loss of commercial electric power supply".

Therefore, in this chapter, to investigate conservativeness of the current evaluation results of DNBR for "Loss of commercial electric power supply" and how the results differ when considering the effects of channel inlet subcooling for CHF, the new CHF correlation of Eq. (8) is adopted to analyze the "Loss of commercial electric power supply" for both JRR-4 and JRR-3.

JRR-4 is a light-water moderated and cooled, graphite reflected pool-type research reactor using HEU plate-type fuel. Its thermal power is 3.5 MW and its averaged heat flux is 0.15 MW/m^2 . A core conversion program from HEU fuel to LEU silicide fuel is currently conducted at JRR-4. JRR-4 reached its initial criticality with LEU

Table 3 Anticipated operational transients analytical results of JRR-4 (Using previous CHF correlations)

Anticipated operational transient	Minimum DNBR	Maximum fuel meat temperature (K)	Maximum fuel surface temperature (K)	Maximum coolant temperature (K)	Thermal stress of fuel plate (kg/mm^2)
Withdrawal of control rods at start-up	3.0	387	385	327	0.36
Withdrawal of control rods at rated power operation	2.8	392	390	329	0.34
Reactivity insertion by removal of irradiation samples	2.5	397	395	329	0.42
Reactivity insertion by cold water insertion to the core	41.1	319	319	314	0.03
Primary pump failure and flow coast-down	2.6	394	393	330	0.31
Secondary pump failure and flow coast-down	2.9	388	386	331	0.31
Loss of commercial electric power supply	1.6	401	400	368	0.31
Safety criterion	>1.5	<673	—	<saturation temperature	<5.7

silicide fuel at July 14, 1998.

JRR-3 is a light-water moderated and cooled, beryllium and heavy-water reflected pool-type research reactor using LEU aluminaide plate-type fuel. Its thermal power is 20 MW and its averaged heat flux is 0.38 MW/m^2 . A core conversion program from aluminaide fuel to silicide fuel is currently being conducted at JRR-3. JRR-3 will start operation with silicide fuel as of 1999.

Figure 9 shows the analytical results of "Loss of commercial electric power supply" at JRR-4, analyzed by using the THYDE-W code⁽¹⁰⁾. In the figure, transients of fuel temperatures, primary coolant temperatures and DNBR are shown until 25 s after the transient begins. DNBRs predicted by both Eqs. (3) and (8) are shown in the figure for a comparison. In JRR-4, there are no auxiliary or emergency pumps for the decay heat removal after coast-down of the primary pumps. Therefore, the core flow reversal occurs just after the primary pumps coast-down. When the transient occurs, the reactor is shut-down by the scram signal of "Loss of power supply", and the core flow decreases due to a coast-down of the primary pumps. The transient is dominated by a competitive process of a decrease in the core flow compared with a decrease in the decay heat after the reactor scram. The minimum DNBRs are calculated during the core flow reversal. Under a steady state condition of JRR-4, a downward coolant velocity is 1.42 m/s. During the transient analysis, DNBR is predicted by Eq. (2) until coolant velocity decreases down to 0.094 m/s. When the coolant velocity is less than 0.094 m/s for downward flow and up to 0.016 m/s after the flow reversal, DNBR is predicted by using Eq. (3). When the coolant velocity is more than 0.016 m/s for upward flow, DNBR is predicted by using Eq. (1). The minimum DNBR during the transient is calculated to be 1.6 and is predicted by using Eq. (3). This analytical result of DNBR is very close to the safety limit of 1.5. On the other hand, the minimum DNBR predicted by using Eq. (8) is 2.2. A difference between 1.6 and 2.2 is due to the effect of channel inlet

subcooling. In this case, the channel inlet subcooling of $\Delta T_{SUB,in}$ is about 70 K and the dimensionless channel inlet subcooling of $\Delta T_{SUB,in}^* [= Cp\Delta T_{SUB,in}/h_{fg}]$ is calculated to be about 0.13. The value of $(1+3\Delta T_{SUB,in}^*)$ is 1.39, therefore, the minimum DNBR predicted by using Eq. (8) is about 1.39 times higher than that predicted by using Eq. (3).

As shown in the above analytical results, the decay heat during core flow reversal is low enough and there is no possibility for the occurrence of the CHF condition. Safety Analysis Report (SAR) has been published based on safety analysis results using the previous CHF correlations of Eqs. (1), (2) and (3). Even using Eq. (3) to predict CHF during the core flow reversal at JRR-4, analytical results show that there is no possibility for the occurrence of CHF condition, but DNBR is very close to the safety limit of 1.5. However, as shown in the analytical results by using the new CHF correlation of Eq. (8), it was made clear that JRR-4 has much more and enough safety margin against CHF in a more realistic condition.

Figure 10 shows analytical results of "Loss of commercial electric power supply" at JRR-3, analyzed by using the THYDE-W code. In the figure, the transients of power, core flow rate and DNBR are shown to be from 178 to 182 min after the transient begins. Under a steady state condition of JRR-3, fuel elements are cooled by a downward flow as well as JRR-4, but the coolant velocity in JRR-3 is much higher than that in JRR-4 and is 5.86 m/s, because of higher heat flux. During the transient analysis of JRR-3, the region boundary velocities of using Eqs. (1), (2) and (3) are different from those in the case of JRR-4 due to different channel configurations such as channel width, heated area etc. DNBR is predicted by Eq. (2) from the steady state condition until the coolant velocity decreases down to 0.082 m/s. When the coolant velocity becomes less than 0.082 m/s, Eq. (3) is used to predict DNBR instead of Eq. (2). Equation (3) is applied until the coolant velocity up to 0.004 m/s after the flow reversal. When the coolant velocity increases more than 0.004 m/s for upward flow, DNBR is predicted

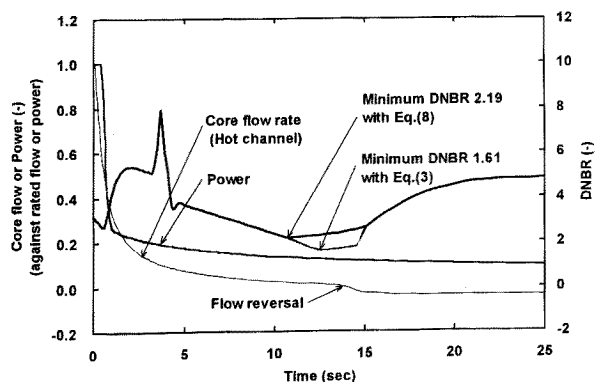


Fig. 9 "Loss of commercial electric power supply" analytical results for JRR-4, comparison of DNBR between predicted by Eqs. (3) and (8)

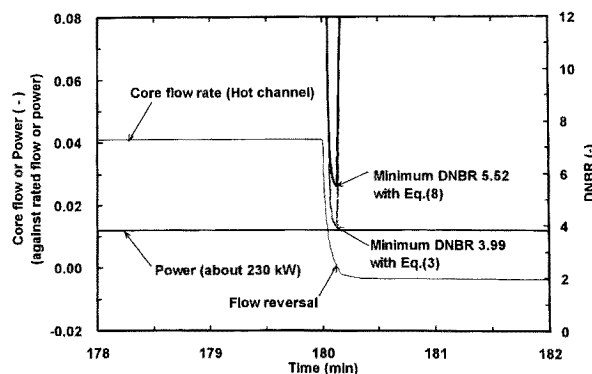


Fig. 10 "Loss of commercial electric power supply" analytical results for JRR-3, comparison of DNBR between predicted by Eqs. (3) and (8)

by using Eq. (1). DNBRs predicted by both Eqs. (3) and (8) are shown in the figure for a comparison. In JRR-3, there are two auxiliary pumps for the decay heat removal after the coast-down of the main primary pumps. In this analysis, one auxiliary pump is assumed to fail at the beginning of the transient to obtain the severest of analysis results. Also, the other auxiliary pump is assumed to stop 180 min after the transient begins by a reactor operator for a long-term core cooling by the natural convection cooling between the reactor core and the reactor pool. Therefore, the core flow reversal occurs just after the auxiliary pump coast-down around 180 min after the transient begins. The minimum DNBR predicted by using Eq. (3) is 4.0, on the other hand that predicted by using Eq. (8) is 5.5. The difference between 4.0 and 5.5 is due to the effect of channel inlet subcooling. In this case, the channel inlet subcooling of $\Delta T_{SUB,in}$ was also about 70 K and the value of $(1+3\Delta T_{SUB,in}^*)$ is 1.39, therefore, the minimum DNBR predicted by using Eq. (8) was about 1.39 times higher than that predicted by using Eq. (3).

Both analytical results of DNBR by using Eqs. (3) and (8) show that the decay heat level is sufficiently low during the core flow reversal and there is no possibility for the occurrence of the CHF condition. As shown in the above analytical results, it was made clear that Eq. (3) predicts 39% smaller CHF than that predicted by Eq. (8) under the condition of the channel inlet subcooling of $\Delta T_{SUB,in}=70$ K. Safety analysis report of JRR-3 silicide core has been published by adopting Eq. (3) to predict CHF, therefore, the 39% corresponds to the conservativeness of the current analysis of JRR-3.

V. Concluding Remarks

The effect of channel inlet subcooling for CHF under the CCFL conditions in rectangular channels, which had not been considered in previous studies, has been investigated based on the CHF experimental data. As a result, it was made clear that CHF in this region increase linearly with an increase of the channel inlet subcooling and Eq. (8) was proposed as a new CHF correlation including the effect of channel inlet subcooling for both uniform and non-uniform heat flux cases. Equation (8) gives a good prediction, allowing the errors of 59% to the upper limit and 40% to the lower limit of the CHF data. For adopting the same criterion regarding CHF to the thermal hydraulic design of research reactors, the confidence level of the Eq. (8) to the CHF data with the deviation of -33% was also investigated by the statistics analysis. The deviation of -33% from Eq. (8) was evaluated to be -1.63 times of the standard deviation (-1.63σ) of the CHF data against Eq. (8). This means that there is a 10% of possibility to occur the CHF condition even when the minimum DNBR is equal to 1.5. Equation (8) could be adopted under the conditions of the atmospheric pressure, the inlet subcooling less than 78 K, the channel gap size between 2.25 to 5.0 mm, the axial peaking factor between 1.0 to 1.6 and L/De between 71 to 174 which were

the ranges investigated in this study. By adopting the new CHF correlation of Eq. (8) to the safety analysis for research reactors of JRR-3 and JRR-4, analytical results show that the current designs of both JRR-3 and JRR-4 have sufficient safety margins against CHF. The conservativeness of current safety analysis results of both JRR-3 and JRR-4 have also been made clear by adopting Eq. (8) to the safety analysis.

[NOMENCLATURE]

- A : Flow area (m^2)
 - A_H : Heated area (m^2)
 - C : Constant in Eq. (7)
 - De : Equivalent hydraulic diameter (m)
 - G : Mass flux ($kg/m^2 \cdot s$)
 - G^* : Dimensionless mass flux $[=G/\sqrt{\lambda(\rho_l - \rho_g)\rho_g g}]$
 - g : Acceleration of gravity (m/s^2)
 - h_{fg} : Latent heat of evaporation (kJ/kg)
 - L : Channel length (m)
 - q_{CHF} : Critical heat flux (CHF) (kW/m^2)
 - q_{CHF}^* : Dimensionless CHF $[=q_{CHF}/h_{fg}\sqrt{\lambda(\rho_l - \rho_g)\rho_g g}]$
 - ΔT_{SUB} : Subcooling (K)
 - ΔT_{SUB}^* : Dimensionless subcooling $[=Cp\Delta T_{SUB}/h_{fg}]$
 - W : Channel width of rectangular channel (m)
 - ρ_g, ρ_l : Density of gas and liquid (kg/m^3)
 - σ : Surface tension (N/m)
 - λ : Critical wave length $[=\{\sigma/(\rho_l - \rho_g)g\}^{1/2}]$
- (Subscripts)
- in : Inlet
 - o : Outlet

—REFERENCES—

- (1) Hirano, M., Sudo, Y.: Analytical study on thermal-hydraulic behavior of transient from forced circulation to natural circulation in JRR-3, *J. Nucl. Sci. Technol.*, **23**[4], 352-368 (1986).
- (2) Sudo, Y., Miyata, K., Ikawa, H., Kaminaga, M., Ohkawara, M.: Experimental study of differences in DNB heat flux between upflow and downflow in vertical rectangular channel, *J. Nucl. Sci. Technol.*, **22**[8], 604-618 (1985).
- (3) Sudo, Y., Kaminaga, M.: A new CHF correlation scheme proposed for vertical rectangular channels heated from both sides in nuclear research reactors, *Trans. ASME, J. Heat Transfer*, **115**, 426-434 (1993).
- (4) Sudo, Y., Ando, H., Ikawa, H., Ohnishi, N.: Core thermohydraulic design with 20% LEU fuel for upgraded research reactor JRR-3, *J. Nucl. Sci. Technol.*, **22**[7], 551-564 (1985).
- (5) Kaminaga, M., Yamamoto, K., Watanabe, S.: Steady-state thermal hydraulic analysis and flow blockage accident analysis of JRR-4 silicide LEU core, *JAERI-Tech* 96-039, (1996), [in Japanese].
- (6) Nagaoka Y., Komukai, B., Sakurai, F., Saito, M., Futamura, Y.: Safety analysis of JMTR-LEU cores (1)—Reactivity initiated accident analysis, *JAERI-M* 92-095, (1992), [in Japanese].
- (7) Mishima, K.: Boiling burnout at low flow rate and low pressure conditions, Dissertation Thesis, Kyoto Univ.,

- (1984).
- (8) Kaminaga, M., Sudo, Y., Murayama, Y., Usui, T.: Experimental study of the critical heat flux in a narrow vertical rectangular channel, *Heat Transfer-Japanese Res.*, **20**[1], 72-85 (1991).
- (9) Kaminaga, M., Sudo, Y.: Experimental study of differences in CHF between upflow and downflow in vertical rectangular channels (Effect of subcooling), *Trans. JSME., Ser. B*, **58**[553], 2799-2804 (1992), [in Japanese].
- (10) Asahi, Y., Matsumoto, K., Hirano, M.: THYDE-W: RCS (reactor-coolant system) analysis code, *JAERI-M* 90-172, (1990).
-